An optimum magnetic control torque generation of a momentum bias satellite

Nurulasikin Mohd Suhadis[1,*], Renuganth Varatharajoo[2]
[1]School of Aerospace Engineering, Engineering Campus,
Universiti Sains Malaysia, 14300 Nibong Tebal,
Pulau Pinang, Malaysia.
[2]Department of Aerospace Engineering, Faculty of Engineering,
Universiti Putra Malaysia, 43400 Serdang,
Selangor, Malaysia.

ABSTRACT

This paper describes a comparison study of magnetic attitude control torque generation performance of a momentum bias satellite operated in Low Earth Orbit (LEO) with various orbit inclinations. The satellite is equipped with two magnetic torquers that are placed along the $+x$ and $+y$ axes where magnetic control torque is generated when these magnetic torquers couple with the geomagnetic fields and its vector direction is perpendicular to both the magnetic fields. The control algorithm was structured using a proportional (P) controller for satellite attitudes/nutation control and a proportional-integral (PI) controller for managing the excess angular momentum on the momentum wheel. The structured control algorithm is simulated for 23°, 53° and 83° orbit inclinations and the generated attitude torque performances are compared to see how the variation of the satellite orbit affects the satellite's attitude torque generation as the magnitude and direction of the geomagnetic fields vary with respect to the altitude and latitude while the magnitude and direction of the magnetic fields generated by the magnetic torquers vary with respect to the orbital motion. Results from simulation show that the higher orbit inclination generates optimum magnetic attitude control torque. Note that this work is the extension of the previous work published in The International Journal of Multiphysics [1].

Keywords: Coupled magnetic fields, magnetic torquer, magnetic attitude control system

1. INTRODUCTION

Momentum bias satellite takes advantage of the gyroscopic stiffness effect provided by the momentum wheel. The nominal angular momentum value generated by the momentum wheel that is placed along the pitch axis not only keeps the pitch axis inertially fixed but it also stiffens the roll/yaw axes thus enabling 3-axis stabilization. However, with a continuous act of external disturbance torques, the gyroscopic stiffness effect is insufficient to maintain high roll/yaw attitude accuracies. This is worsening by the nutation effect induced on the momentum wheel and the momentum wheel itself cannot independently remove its accumulated angular momentum which eventually gets saturated [2]. Therefore, an

*Corresponding author; Email: normatsue@yahoo.com

additional actuator is necessary on this type of satellite in order to eliminate those drawbacks thus achieving a high pointing accuracy along all the three axes. As for the mission operated in Low Earth Orbit (LEO), magnetic torquer has been a primary option in dealing with these issues as the strength of the geomagnetic field is relatively high within LEO and the magnetic torque itself is lightweight, requires low power consumption and inexpensive.

Magnetic torque is generated when magnetic field generated by magnetic torquer couples with the geomagnetic fields where its vector direction is perpendicular to both the magnetic fields. In a system developed by Fan et al. [3] , two magnetic torquers were used and aligned along the roll and yaw axes where controllers were developed based on the PD controller. Each of these magnetic torquers was used to control any roll/yaw axis that was normal to them while the momentum unloading was achieved by both magnetic torquers. Similar control strategy and controller were also adopted by Lv et al. [4]. The only difference between these two works is on the control gains optimization method. The former used multiobjective optimization approach while the latter used genetic algorithms (GA) method. It was proven from simulations that these two proposed optimized control gains design demonstrated high pointing and stability accuracies. The UoSat-12 [5] and SNAP-1 [6-7] were amongst the satellite built by SSTL that employing three magnetic torquers for attitude acquisition, nutation damping and momentum unloading purposes. Therefore, the developed control scheme for these satellites is quite similar. During the attitude acquisition phase, the magnetic torquer along the pitch axis was used to reduce the roll/yaw angular rates first, then the magnetic torquer along the roll/yaw axis was used for controlling the pitch angular rate thus bringing it to a Y-Thomson mode of stabilization for the momentum wheel start-up. While during the nadir pointing phase, the magnetic torquer cross-product control law was used for the nutation control and the wheel momentum unloading. The first Algerian microsatellite called Alsat-1 was also built with the collaboration with SSTL. This satellite opted to use the reaction wheel for a fine yaw pointing during the nadir pointing phase [8]. Therefore, the magnetic torquers were only used for the nutation and momentum unloading controls. The control algorithm for the attitude acquisition phase was similar with the one implemented on the UoSat-12 and SNAP-1 missions. While during the nadir pointing phase, the algorithm was slightly different due to the employment of the reaction wheel. The in-orbit results for this satellite obtained from the ground station demonstrate the operation success of the satellite pointing requirements [9-10]. For a nanosatellite developed by graduate students at the Hankuk Aviation University called HAUSAT-2, only the magnetic torquer along the pitch axis was used during the nominal mode for the roll/yaw control in order to avoid any interference with the pitch axis control. The momentum dumping of the wheel was accomplished using the magnetic torquer along the roll and pitch axes. Due to the mission power constraint, the momentum dumping process was proposed not to be operated in a continuous mode. Instead, the specific angular momentum value was set as a boundary where the dumping process was only performed when this boundary value is exceeded. Despite this intermittent control, simulations performed showed that this approach satisfies the attitude mission requirements. Another research based on the three magnetic torquers was carried out by Chen et al. [11]. In their work, the ACS system for a small satellite equipped with reaction wheels and magnetic torquers was considered. In the case of a reaction wheel failure along the roll and yaw axis, a strategy to alter the reaction wheel along the pitch axis to a momentum wheel then combined with three magnetic torquers in order to provide the 3-axis stabilization. To accomplish the wheel start-up, the momentum unloading algorithm based on the magnetic torque cross-product control law was developed in order to unload the excessive wheel momentum.

In this paper, the system described in [1] and [12] will be simulated for 23°, 53° and 83° orbit inclinations and the generated attitude torque performances during nominal attitude operation along these orbits will be compared to see how the variation of the satellite orbit affects the satellite's attitude torque generation as the magnitude and direction of the geomagnetic fields vary with respect to the altitude while the magnitude and direction of the magnetic fields generated by the magnetic torquers vary with respect to the orbital motion. The system is equipped with two magnetic torquers that are aligned along the roll and pitch axes where they are used for momentum unloading and controlling roll/yaw attitude/nutation, respectively.

2. MISSION CONFIGURATION

The satellite mission for this work is nadir pointing and its configuration is depicted in Figure 1. The momentum wheel along the -*y* axis is used to provide gyroscopic stiffness along this axis. The magnetic torquer along the +*x* axis is used for momentum unloading while the magnetic torquer along the +*y* axis is for controlling roll/yaw attitude and nutation. Lastly, the gravity gradient boom that is extended along the -*z* axis is to increase the moment of inertia along the *x* and *y* axes axis, thus, giving the gravity gradient stabilization along the *z* axis. Note that for nadir pointing mission, the *z* axis points toward the earth, the *y* axis is normal to the orbital plane and the *x* axis points toward the satellite's orbital motion and complete the right-hand orthogonal system.

Based on this configuration, the linearized dynamic equation of motion of the satellite along roll and yaw axes defined for the attitude and nutation are as follow

$$\begin{bmatrix} \dot{h}_{0x} \\ \dot{h}_{0z} \end{bmatrix} = \begin{bmatrix} 0 & \omega_0 \\ -\omega_0 & 0 \end{bmatrix} \begin{bmatrix} h_{0x} \\ h_{0z} \end{bmatrix} + \begin{bmatrix} 1 & 0 \\ 0 & 1 \end{bmatrix} \begin{bmatrix} T_x \\ T_z \end{bmatrix} \tag{1}$$

$$\begin{bmatrix} \dot{\omega}_x \\ \dot{\omega}_z \end{bmatrix} = \begin{bmatrix} 0 & -h_{wy}/I_x \\ h_{wy}/I_x & 0 \end{bmatrix} \begin{bmatrix} \omega_x \\ \omega_z \end{bmatrix} + \begin{bmatrix} 1/I_x & 0 \\ 0 & 1/I_z \end{bmatrix} \begin{bmatrix} T_x \\ T_z \end{bmatrix} \tag{2}$$

where h_{ox} and h_{oz} are roll and yaw angular momentum, ω_x and ω_y are satellite's body angular velocity components, ω_o is orbital frequency and h_{wy} is wheel bias momentum. Note that the momentum wheel gives the perfect attitude pointing along the pitch axis [13], therefore, only controlling the angular momentum value of the momentum wheel is of interest herein. The linearized equation along the pitch axis only considering the angular momentum of the wheel is written as follows

$$\begin{bmatrix} \dot{h}_{wy} \end{bmatrix} = [1] \begin{bmatrix} T_y \end{bmatrix} \tag{3}$$

The external torque T_x, T_y and T_z in Eq. (1), Eq. (2) and Eq. (3) consists of two essential parts which are the disturbance torque and the control torque. Their relation can be defined as follows

$$\begin{bmatrix} T_x \\ T_y \\ T_z \end{bmatrix} = \begin{bmatrix} T_{dx} + T_{mx} \\ T_{dy} + T_{my} \\ T_{dz} + T_{mz} \end{bmatrix} \tag{4}$$

Table 1: Satellite parameters

Parameter	Value
Weight	50 *Kg*
Dimension	690 × 366 × 366 *mm*
I_x	178 Kgm^2
I_y	181 Kgm^2
I_z	4.3 Kgm^2
h_{wy}	8.04 *Nms*
$M_{magnetic\ torquer}$	15 Am^2
Input	$T_{dx} = 12.8\times10^{-6} + 8.6\times10^{-6}\sin(\omega_0 t)\,Nm$ $T_{dy} = 55\times10^{-6} + 55\times10^{-6}\sin(\omega_0 t)\,Nm$ $T_{dz} = 12.8\times10^{-6} + 4.3\times10^{-6}\sin(\omega_0 t)\,Nm$
Initial conditions	$\phi(0) = 5°$, $\theta(0) = 5°$, $\psi(0) = 5°$ $\omega_x(0) = 0$, $\omega_z(0) = 0$

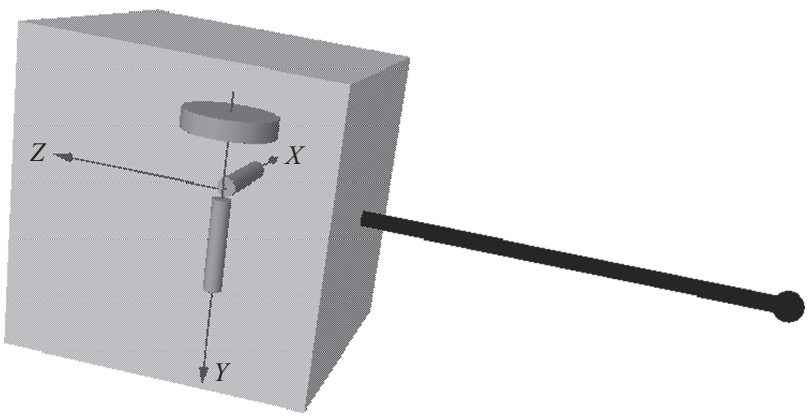

Figure 1: Satellite configuration

In this work, the disturbance torque consists of the gravity gradient torque T_{gg}, aerodynamic torque T_{aero}, magnetic torque $T_{magnetic}$ and solar radiation torque T_{solar}, while the control torque is generated by the onboard magnetic torquers. Details of satellite parameters is described in Table 1.

3. MAGNETIC CONTROL TECHNIQUE

The magnetic control torque, $\mathbf{T}_m$ is induced when the magnetic fields generated by the magnetic torquers onboard satellite, **M** couple with the geomagnetic fields, **B** whereby the vector of the generated torque is constrained to be perpendicular to both the magnetic fields. This interaction is mathematically described as

$$\mathbf{T}_m = \mathbf{M} \times \mathbf{B} \tag{5}$$

The required magnetic field need to be generated by the magnetic torquer is calculated based on the following equation

$$\mathbf{M} = -\frac{\mathbf{k}}{B^2}(\mathbf{B} \times \Delta\mathbf{h}) \tag{6}$$

where **K** is the unloading control gains. Then, the total magnetic control torque can be defined by inserting Eq. (6) into Eq. (5)

$$\mathbf{T}_m = -\frac{\mathbf{k}}{B^2}(\mathbf{B} \times \Delta\mathbf{h}) \times \mathbf{B} \tag{7}$$

As the magnetic field vector components expressed in the reference coordinate system along 23°, 53° and 83° orbit inclinations are non-zero, there will be a direct coupling between the roll and yaw angular momentums for the existing magnetic torquers. Therefore, decoupling matrix is introduced to eliminate this effect and a filter for the wheel momentum control is used in order to minimize the impact of the momentum wheel control action on the roll/yaw control. Therefore, with these strategies, the magnetic torquer along the pitch axis is strictly used for controlling roll/yaw axes while the magnetic torquer along the roll axis is for the wheel momentum unloading. Based on this strategy, the magnetic dipole moment need to be generated for attitude and nutation control are as follow

$$M_y = -\frac{B_z A_{21}}{B^2} h_{0x},\ M_x = -\frac{B_y A_{13}}{B^2} h_{0z} \tag{8}$$

$$M_y = -\frac{B_z N_{21}}{B^2} \omega_x + \frac{B_x N_{22}}{B^2} \omega_z \tag{9}$$

While the magnetic dipole moment needs to be generated for momentum unloading is as follow

$$M_x = -\frac{B_z A_{12}}{B^2} \left(\frac{k_p \bullet s + 1}{s} \right) \Delta h_w \tag{10}$$

The values of the geomagnetic field magnitude along the orbit can be defined by a series of spherical harmonics as follow [14],

$$V(r,\theta,\lambda) = R \sum_{n=1}^{k} \left(\frac{R}{r} \right)^{n+1} \sum_{m=0}^{n} \left(g_n^m \cos m\lambda + h_n^m \sin m\lambda \right) P_n^m(\theta) \tag{11}$$

where R is the equatorial radius of the earth, (r, θ, λ) are the geocentric distance, co-latitude and east longitude from Greenwich,(g_n^m, h_n^m) are the Schmidt normalized Gaussian coefficients and $P_n^m(\theta)$ is the associated Legendre functions. There two available main models of Gaussian coefficients that are available are the International Geomagnetic Reference Field (IGRF) and the World Magnetic Model (WMM). In this work, the IGRF model has been chosen. The general solution of this function expressed in spherical coordinate system can be written as follows

$$B_r = \sum_{n=1}^{k} \left(\frac{R}{r} \right)^{n+2} (n+1) \sum_{m=0}^{n} \left(g^{n,m} \cos m\lambda + h^{n,m} \sin m\lambda \right) P^{n,m}(\theta) \tag{12}$$

$$B_\theta = -\sum_{n=1}^{k} \left(\frac{R}{r} \right)^{n+2} \sum_{m=0}^{n} \left(g^{n,m} \cos m\lambda + h^{n,m} \sin m\lambda \right) \frac{\partial P^{n,m}(\theta)}{\partial \theta} \tag{13}$$

$$B_\lambda = \frac{-1}{\sin\theta}\sum_{n=1}^{k}\left(\frac{R}{r}\right)^{n+2}\sum_{m=0}^{n} m\left(-g^{n,m}\sin m\lambda + h^{n,m}\cos m\lambda\right)P^{n,m}(\theta) \tag{14}$$

In the satellite application, the magnetic field data are conveniently expressed in the Earth-Centered Inertial (ECI) coordinate frame. The transformation of the data from Right Ascension-Declination coordinate frame to ECI coordinate frame can be defined as follow

$$\mathbf{B}_{ECI} = \begin{bmatrix} (B_r\cos\delta + B_\theta\sin\delta)\cos\alpha - B_\lambda\sin\alpha \\ (B_r\cos\delta + B_\theta\sin\delta)\sin\alpha - B_\lambda\cos\alpha \\ (B_r\sin\delta - B_\theta\cos\delta) \end{bmatrix} \tag{15}$$

However, in this work the geomagnetic field value defined by Eq. (15) are transformed into Local Vertical Local Horizontal (LVLH)

$$\mathbf{B}_{LVLH} = \left[\mathbf{A}(\mathbf{q})\right]\mathbf{B}_{ECI} \tag{16}$$

Where **A** (**q**) is a transformation matrix defined as follow

$$\left[\mathbf{A}(\mathbf{q})\right] = \begin{bmatrix} q_1^2 - q_2^2 - q_3^2 + q_4^2 & 2(q_1q_2 + q_3q_4) & 2(q_1q_3 - q_2q_4) \\ 2(q_1q_2 - q_3q_4) & -q_1^2 + q_2^2 - q_3^2 + q_4^2 & 2(q_2q_3 + q_1q_4) \\ 2(q_1q_3 + q_2q_4) & 2(q_2q_3 - q_1q_4) & -q_1^2 - q_2^2 + q_3^2 + q_4^2 \end{bmatrix} \tag{17}$$

Based on the parameters described in Table 2, values of the geomagnetic field for 23°, 53° and 83° orbit inclinations have been generated and plotted in Figure 1. The B_x and B_z components vary with respect to the orbital motion as these two components are measured along the $+x$ and $+z$ axis of the LVLH coordinate system which are lying in the orbital plane. Whereas the B_y component is measured along the $+y$ axis which is normal to the orbital plane and only influenced by the rotation of the earth. It is also shown that the magnitude of the geomagnetic field is stronger over the pole and weaker over the equatorial.

Table 2: Orbital parameters

Parameters	**Value**
Altitude, h	540 *Km*
Inclination, t	53°
Eccentricity, e	≈ 0
Right ascension of ascending node, Ω	0°
Argument of perigee, ω	0°
True anomaly, v	0°
Simulation time, t	5 orbits
Epoch	1 April 2010
Orbital frequency, ω_o	0.0011 $rads^{-1}$

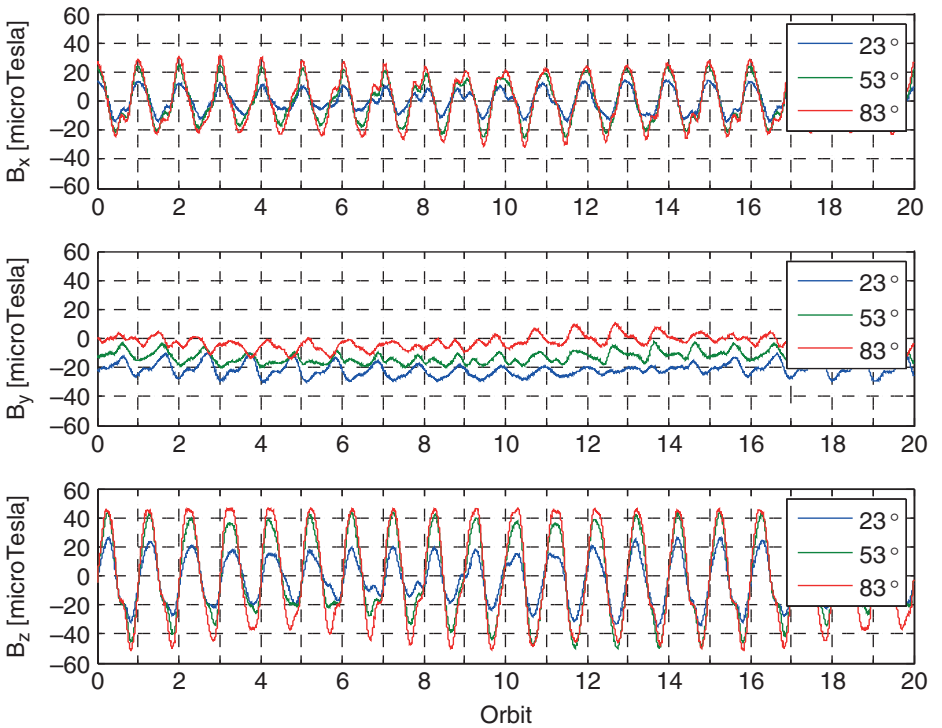

Figure 2: Comparison of the geomagnetic field models along 23°, 53° and 83° orbit inclinations

4. NUMERICAL TREATMENTS

Series of simulations have been performed to see the attitude torque generation performances along the 23°, 53° and 83° orbit inclinations. Simulations are performed using the MATLAB® SIMULINK® software. Details of the satellite parameters and orbital parameters are given in Tables 1 and 2, respectively. Note that, the tuning of the control gains is based on the geomagnetic field values along the 53° orbit inclination and the same gains are later used to simulate the performance along the 23° and 83° to see the effect of varying the orbit inclination. Detail values of gains are given in Table 3.

Table 3: Control parameters

Attitude gains	$A_{13} = -0.002$ $A_{21} = -0.002$
Nutation gains	$N_{21} = -1.2$ $N_{22} = 1.2$
Momentum unloading gains	$A_{12} = k_i$ $k_i = \omega_n^2$ $k_p = \frac{2\xi}{\omega_n}$ $\omega_n = 4 \times 10^{-3}$ $\xi = 1$

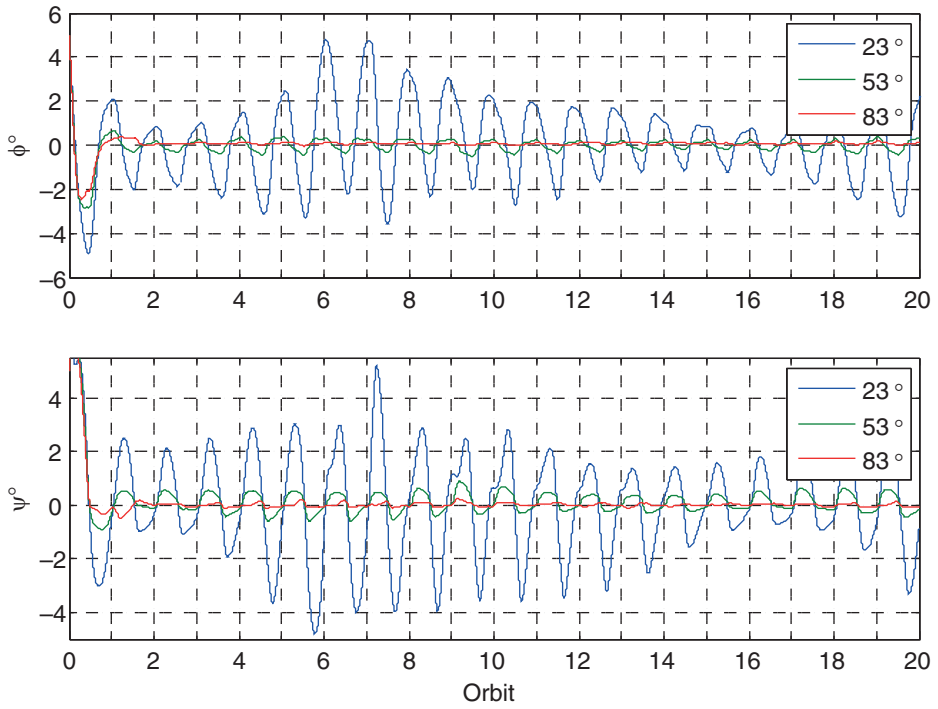

Figure 3: Comparison of the attitude performance

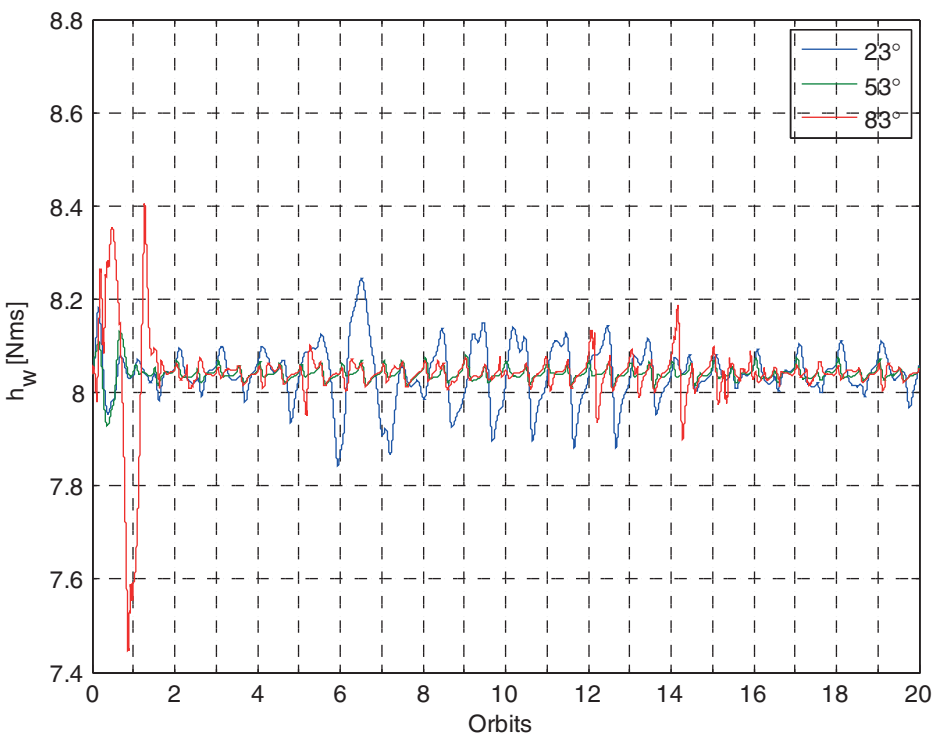

Figure 4: Comparison of the angular momentum performance

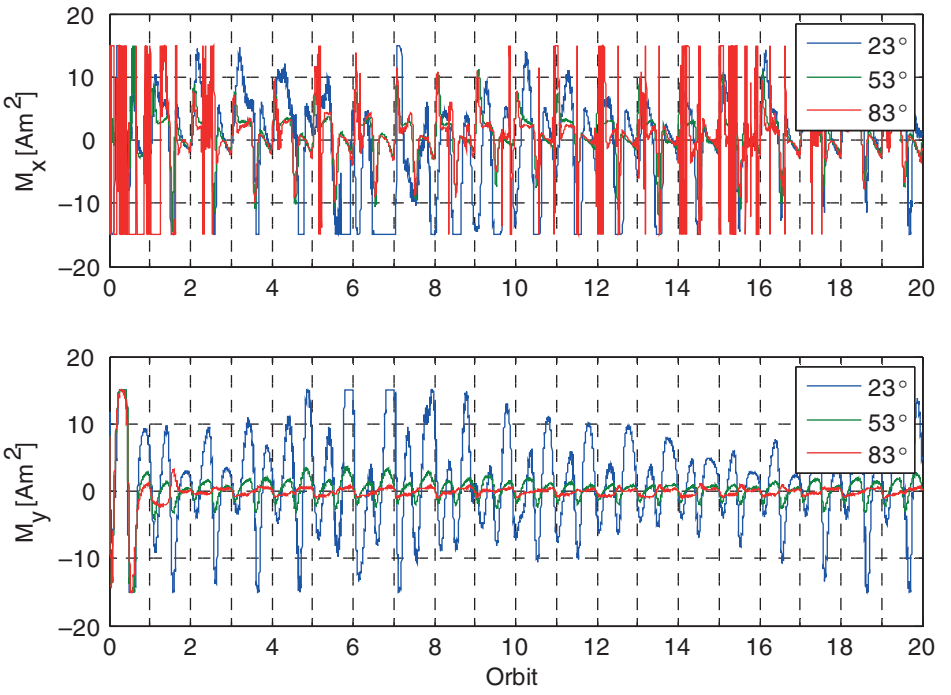

Figure 5: Comparison of the magnetic dipole moment generation

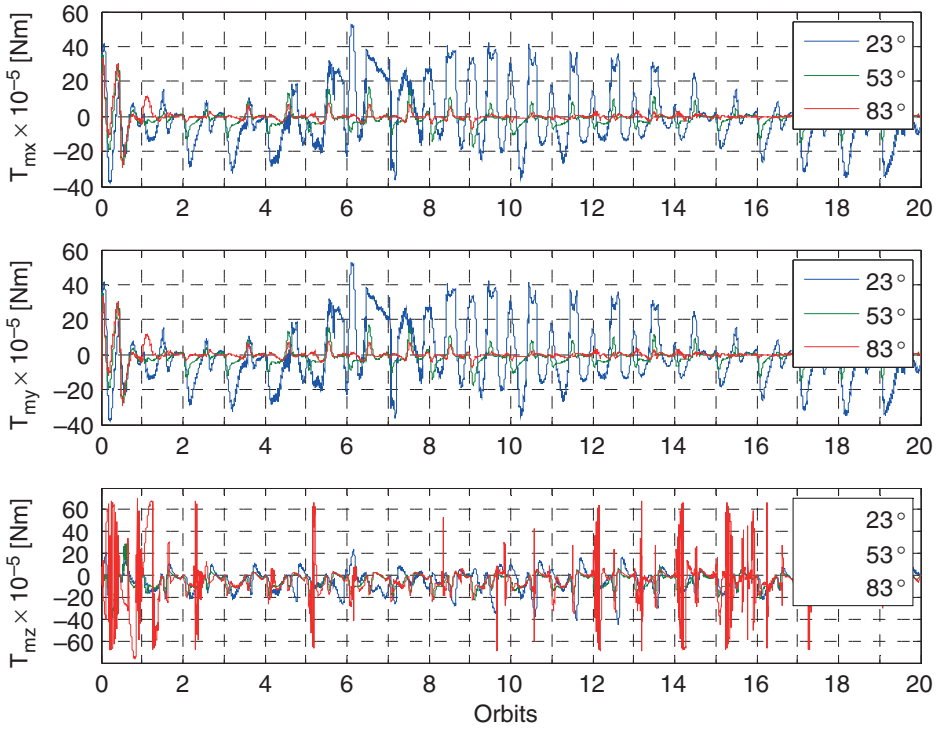

Figure 6: Comparison of the magnetic control torque generation

The roll and yaw attitude performances are depicted in Figure 3. The plots show that the roll axis oscillates with and accuracy between 0° and 0.15° for 83° orbit inclination, between –0.5° and 0.4° for 53° orbit inclination and between –4° and 4° for 23° orbit inclination. Meanwhile, the yaw axis oscillates with and accuracy between –0.1° and 0.15° for 83° orbit inclination, between –0.6° and 0.9° for 53° orbit inclination and between –5° and 5.5° for 23° orbit inclination. It can be clearly seen that the attitude performance of the satellite improves as the orbit increases. This is actually reflects the geomagnetic field values that is stronger over the pole and weaker over the equatorial. Figure 4 shows the comparison of the angular momentum unloading performance. The performance along the 83° orbit inclination reaches steady state error after 1.5 orbits while along the 23° and 53° orbit inclinations, they take only half orbit with a tight momentum control within the 8.04 Nms vicinity. These attitude and momentum unloading performances are achieved with magnetic dipole moments generated by each magnetic torque onboard as shown in Figure 5 and the torque generated along the roll, pitch and yaw axes are shown in Figure 6.

5. CONCLUSION

In this paper, the control torque generation of a momentum bias satellite employing magnetic torquers onboard has been simulated for 23°, 53° and 83° orbit inclinations to see how the orbit inclination variation affects the magnetic control torque generation. The control algorithm was structured where the magnetic torque along the roll axis is used for momentum unloading while the magnetic torque along the pitch axis is used for roll/yaw attitude/nutation control. Simulations were performed using the MATLAB® SIMULINK® codes. Results from the simulations show that the higher orbit inclination generates optimum magnetic attitude control torque for this satellite configuration.

ACKNOWLEDGEMENT

The work presented in this paper has been supported by the Exploratory Research Grant Scheme (203/PAERO/6730062).

REFERENCES

[1] N.M. Suhadis and R. Varatharajoo, A Study of Coupled Magnetic Fields for an Optimum Torque Generation, *The International Journal of Multiphysics*, Vol. 6 (1), 73–88, 2012.

[2] K. Tsuchiya, M. Inoue, N. Wakasuqi, and T. Yamaguchi, Advanced reaction control wheel controller for attitude control of spacecraft. *Acta Astronautica*, 1982, 9(12), 697–702.

[3] Z. Fan., S. Hua, M. Chundi, and L. Yuchang, An optimal attitude control of small satellite with momentum wheel and magnetic torquers. *Proceedings of the 4th World Congress on Intelligent Control and Automation*, China, 2001.

[4] J. Lv, G. Ma, and D. Gao, Bias momentum satellite magnetic attitude control based on genetic algorithms, *UKACC International Conference on Control*, 2006.

[5] W.H. Steyn, and Y. Hashida, An attitude control system for a low-cost earth observation satellite with orbit maintenance capability, *13th AIAA/USU Conference on Small Satellites*, 1999.

[6] W.H. Steyn, Y. Hashida, and V. Lappas, An attitude control system and commissioning results of the SNAP-1 nanosatellite. *14th AIAA/USU Conference on Small Satellites*, 2000.

[7] W.H. Steyn, and Y. Hashida, In-orbit Attitude Performance of the 3-Axis Stabilized SNAP-1 Nanosatellite. *15th AIAA/USU Conference on Small Satellites*, 2001.

[8] A.M. Mohammed , An attitude determination and control system of the Alsat-1 first Algerian microsatellite. *Proceedings of the IEEE Recent Advances in Space Technologies RAST'03*, Istanbul, Turkey, 2003, 162–167.

[9] A.M. Mohammed, M. Benyettou, M.N. Sweeting, and J.R. Cooksley, Initial Attitude Acquisition Result of the Alsat-1 First Algerian Microsatellite in Orbit, *IEEE International Conference on Networking, Sensing and Control*, Tucson, AZ, USA, 2005, 566–571.

[10] A.M. Mohammed , M. Benyettou , Y. Bentoutou , A. Boudjemai, Y. Hashida and M.N. Sweeting, Three-axis active control system for gravity gradient stabilised microsatellite. *Acta Astronautica*, 2009, 64(7-8), 796–809.

[11] M. Chen, S.J. Zhang, F.H. Liu, and Y.C. Zhang, Combined attitude control of small satellite using one flywheel and magnetic torquers. *2nd International Symposium on Systems and Control in Aerospace and Astronautics*, 2008, 1–6.

[12] J. Bals, W. Fichter, and M. Surauer, Optimization of magnetic attitude and angular momentum control for low earth orbit satellites. *Proceedings Third International Conference on Spacecraft Guidance, Navigation and Control Systems*, ESTEC, Noordwijk, The Netherlands, 1996.

[13] R. Varatharajoo, and S. Fasoulas, The combined energy and attitude control system for small satellites – Earth observation mission. *Acta Astronautica*, 2005, 56(1-2), 251–259.

[14] S. McLean, S. Macmillan, S. Maus, V. Lesur, A. Thompson and D. Dater, The US/UK World Magnetic Model for 2005-2010, *NOAA Technical Report NESDIS/NGDC-1*, 2004.